

UNCLASSIFIED

AD NUMBER

AD814674

LIMITATION CHANGES

TO:

Approved for public release; distribution is unlimited. Document partially illegible.

FROM:

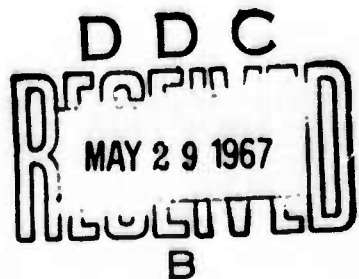
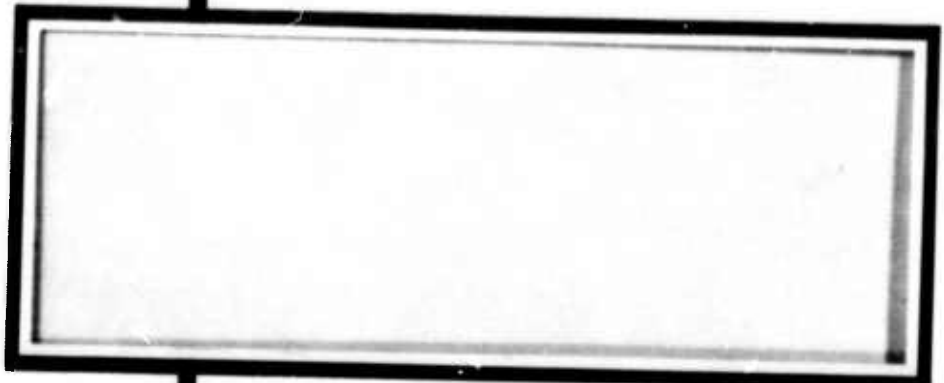
Distribution authorized to U.S. Gov't. agencies and their contractors; Critical Technology; FEB 1967. Other requests shall be referred to Air Force Technical Application Center, Washington, DC 20333. Document partially illegible. This document contains export-controlled technical data.

AUTHORITY

usaf ltr, 25 jan 1972

THIS PAGE IS UNCLASSIFIED

AD814674



STATEMENT #2 UNCLASSIFIED

This document is subject to special export controls and each transmittal to foreign government or foreign nationals may be made only with prior approval of U.S. AETAC, Washington, D.C. 20333

SCIENCE SERVICES DIVISION

TEXAS INSTRUMENTS
INCORPORATED



ARRAY RESEARCH
STUDY OF TELESEISMS RECORDED AT
CUMBERLAND PLATEAU OBSERVATORY
SPECIAL REPORT NO. 25

Prepared by

Robert B. Roden

John P. Burg, Project Scientist

TEXAS INSTRUMENTS INCORPORATED
Earth Science Programs
P. O. Box 5621
Dallas, Texas 75222

Contract AF 33(657)-12747

Date: 13 November 1963

Expiration Date: 20 January 1967

Prepared for

AIR FORCE TECHNICAL APPLICATIONS CENTER
VELA SEISMOLOGICAL CENTER
Washington, D.C. 20333

ARPA Order 104-60
Project Code 8100

28 February 1967



TABLE OF CONTENTS

Section	Title	Page
I	INTRODUCTION	1
II	CONVENTIONAL ANALYSIS OF TELESEISM RECORDINGS	3
III	CRUSTAL REVERBERATION DECONVOLUTION	5
IV	DEPTH-OF-FOCUS DETERMINATION	13
V	STUDY OF CPO CRUSTAL STRUCTURE	17
VI	INVESTIGATION OF PROPAGATION MECHANISMS	27
VII	COMPARISON OF PROCESSORS AT CPO	33/34
VIII	CONCLUSIONS	35/36
IX	REFERENCES AND BIBLIOGRAPHY	37/38

LIST OF ILLUSTRATIONS

Figure	Title	Page
1	S/N Ratios Computed for Center Seismometer and Processor Output (Event II-5)	2
2	Average Power Spectrum of 60 Ensemble II Teleseisms	7
3	Original and Deconvolved Recordings of Event I-4 (1.5-cps High-Cut Playback Filter Applied)	8
4	Original and Deconvolved Recordings of Four Events (1.5-cps High-Cut Playback Filter Applied)	9
5	Impulse Responses of Ensemble-Average Deconvolution Operators	10
6	High-Cut-Filtered Autocorrelations of Original and Deconvolved Records of Event I-4, with Observed and USC&GS-Predicted P-pP Intervals Indicated	14
7	Average Autocorrelations of Subgroups of Ensemble I Events	18



LIST OF ILLUSTRATIONS (CONTD)

Figure	Title	Page
8	Signal Power Spectra of 18 Ensemble II Events Between 20° and 30°	19
9	Noise Power Spectra Associated with 18 Ensemble II Events Between 20° and 30°	20
10	Signal Power Spectra of Seven Deep-Focus Events Between 30° and 31.3°	21
11	Autocorrelations of Four Teleseismic Signals from Earthquakes Near the Colombia-Venezuela Border	22
12	Model of Crustal Structure Near McMinnville, Tennessee	24
13	Travel Paths of Reflected Arrivals	25
14	Smoothed Average Power Spectra of Ensemble III Events Grouped According to Distance	28
15	Ray Paths of Compressional Waves in the Earth's Core and Mantle	30
16	Smoothed Average Power Spectra of Circum-Pacific Events Grouped According to Source Region	31

LIST OF TABLES

Table	Title	Page
1	Description of CPO Teleseism Ensembles	2
2	Results of Conventional Analysis of CPO Teleseism Ensembles	4
3	Descriptions of Teleseisms Displayed in Deconvolution Study	6
4	Computed Lag Times of Reflected Arrivals	26
5	Circum-Pacific Earthquakes	32



SECTION I

INTRODUCTION

During 1963, Multiple Array Processor (MAP) systems were operated online at the 19-element Cumberland Plateau Observatory (CPO) array in order to enhance the teleseismic P-waves relative to surface-wave noise. Outputs of these processors and of the individual seismometers were recorded in analog format on magnetic tape and photographic film. Subsequently, three ensembles of selected recordings were digitized for computer analysis at 50-msec intervals, with later resampling of Ensembles II and III at 100 msec. The transcribed records are 4 min long, with start times chosen so that the P onset is approximately at the center of the record.

The MAP systems were isotropic processors designed to reject low-velocity noise and preserve high-velocity signals with a minimal dependence on azimuth. The outputs contain relatively clean bodywave signals, since the processors attenuate both ambient noise and signal-generated noise (energy scattered into surface waves in the vicinity of the receiver). For the study of analytical techniques such as autocorrelation, deconvolution and pP depth-of-focus estimation, it is advantageous to have records with higher signal-to-noise ratios than could be obtained from a single seismometer. Figure 1 shows, for a representative event, the improvement due to the MAP processing.

Table 1 gives a description of the three ensembles of teleseisms. Ensembles I and II were recorded during the operation of processor IP-8⁸ which was designed from a theoretical signal model and an experimentally measured noise model; the processor contained a low-cut frequency filter for elimination of microseisms with 6-sec period. Processor TIP or IP-1^{6,7} produced the recordings of Ensemble III. Since a theoretical noise model (later found to be inaccurate) was used in the design, TIP was less effective than IP-8 in rejecting the noise actually encountered at CPO; therefore, the records of Ensembles I and II are generally of better quality than those of Ensemble III.

An outline of the investigation and results will be presented in this report. More detailed descriptions may be found in Semiannual Technical Reports prepared by Texas Instruments Incorporated for Air Force Technical Applications Center under Contract AF 33(657)-12747.¹⁰

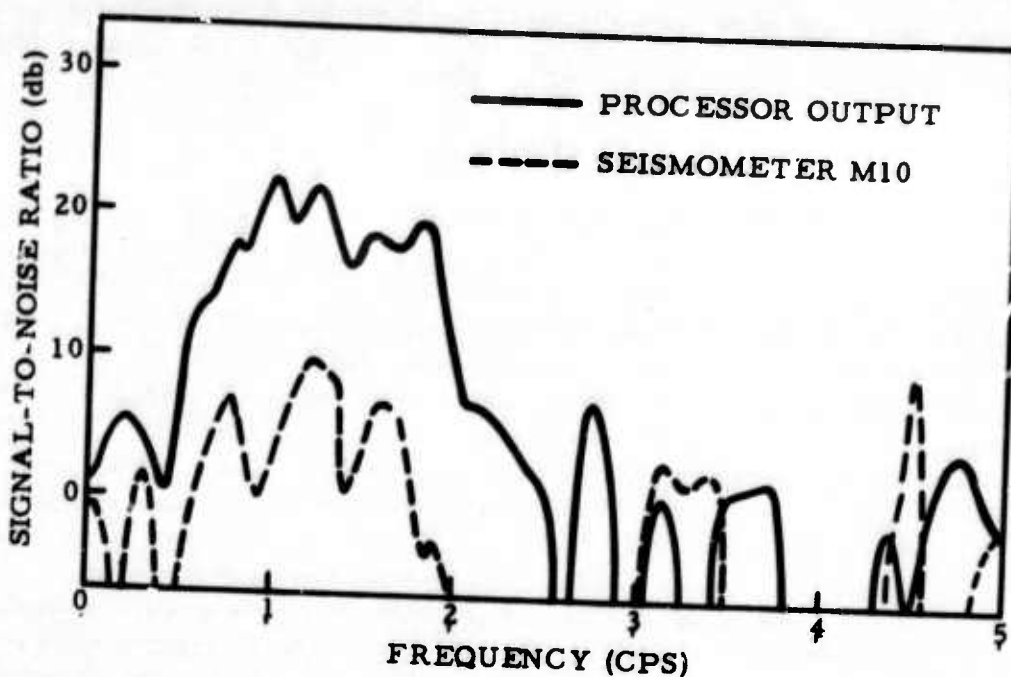


Figure 1. S/N Ratios Computed for Center Seismometer and Processor Output (Event II-5)

Table 1
DESCRIPTION OF CPO TELESEISM ENSEMBLES

	Ensemble I	Ensemble II	Ensemble III
Total Number of Events Digitized	196	71	150
Number of Events Used in Computer Analysis	73	60	119
Geographic Distribution	Kurile Islands Region Only	Worldwide Except Kurile Islands Region	Worldwide
Time of Recording	September, October 1963	September, October 1963	February-May 1963
Processor in Operation	"Experimental" IP-8	"Experimental" IP-8	"Theoretical" IP-1



SECTION II

CONVENTIONAL ANALYSIS OF TELESEISM RECORDINGS

Event parameters measured from the film records are compared in Table 2 with values published by the United States Coast and Geodetic Survey (USC&GS) in Preliminary Determination of Epicenters (PDE) bulletins. The tabulated values of the probable errors are the ranges within which 50 percent of the individual observations lay.

Observed arrival times were compared with arrival times computed from Jeffreys-Bullen⁵ travel-time tables and PDE-published origin times and epicentral coordinates. The greater scatter of residuals observed for the worldwide ensembles, as compared to Ensemble I, suggests that the station correction may depend upon azimuth and/or range. The average delay of 0.3 sec for the Kurile Islands ensemble is clearly not typical of all observed events. Azimuthal variations of station residuals have been observed by Cleary and Hales.¹ An alternative explanation is that source corrections and PDE errors are probably more variable in the worldwide ensembles because of the greater differences in source environment and in station coverage used to define PDE values. It is obviously not possible to define a universal CPO station correction from these results.

Magnitudes were computed from the USC&GS formula

$$m_b = \log \frac{A}{T} + Q + S$$

where

m_b = magnitude

A = maximum amplitude (microns) of the first few cycles of P

T = apparent period at the time corresponding to A

S = station correction factor (assumed zero)

Q = attenuation factor depending upon range and focal depth²

Computed magnitudes averaged 0.2 units lower than those published by USC&GS. At least part of this effect is probably due to signal degradation by the MAP system at some frequencies. Station-to-station variations in crustal transmission properties require station magnitude corrections as large as the observed discrepancy; therefore, the value 0.2 must be regarded as a magnitude correction for the combined effects of station environment and processor.



Table 2
RESULTS OF CONVENTIONAL ANALYSIS
OF CPO TELESEISM ENSEMBLES

	Ensemble I	Ensemble II	Ensemble III
Observed Minus USC&GS Predicted P Arrival Times (sec)	0.3 ± 0.4 (185 events)	0.1 ± 0.9 (68 events)	-0.3 ± 0.9 (150 events)
Observed Minus USC&GS Published Magnitudes (m_b)	-0.3 ± 0.2 (183 events)	-0.3 ± 0.3 (59 events)	-0.1 ± 0.4 (136 events)
(P - pP) Depth of Focus Minus USC&GS Published Depth (km) — Including Uncertain pP Observations	-3 ± 5 (147 events)	-2 ± 7 (32 events)	-3 ± 10 (53 events)
(P - pP) Depth of Focus Minus USC&GS Published Depth (km) — Probable pP Observations Only	-1.9 ± 5.1 (120 events)	1.9 ± 5.7 (6 events)	-5.1 ± 9.6 (17 events)
Detectability of pP Phase — Probable and Uncertain Observations	150 of 196	32 of 71	60 of 174
Detectability of pP Phase — Probable Observations Only	125 of 196	13 of 71	24 of 174

Phases pP or pPKP were sought and the existence of an observable surface-reflected phase on each record was evaluated as "probable", "uncertain" or "negative". For each event for which pP (or pPKP) could be identified, focal depth was computed from the time difference between P and pP (or PKP and pPKP). When all observations were included, these depths averaged 3 km shallower than USC&GS-published values for all ensembles—a result which suggests that the USC&GS method of epicenter determination may be biased slightly toward deep focal depth. The analysis was repeated using only "probable" reflected phases and eliminating all events with the published depth of 33 km, since this value usually implies that no satisfactory estimate of focal depth could be obtained from travel times. An average discrepancy of 2 km remained.



SECTION III

CRUSTAL REVERBERATION DECONVOLUTION

An impulsive P-wave signal emerging from the mantle encounters a series of reflecting interfaces. The result of combining the signal reverberations is equivalent to the effect of a frequency filter which converts the impulse into a wavelet of theoretically infinite duration. In practice, the wavelet's time span is finite since the amplitude cannot remain indefinitely above detection threshold. It is desirable to design an inverse filter which operates on the observed signal in such a way as to remove crustal effects by transforming the waveform back to an impulse.

If deconvolution filters are designed from experimentally observed signals, the nature of the filters will depend upon the signal spectra at the receiving station. In general, such spectra will depend on crustal effects to a much lesser degree than on signal spectra incident at the bottom of the crust; these incident signal spectra depend on both source spectra and mantle transmission effects (including anelastic absorption). Thus, the major effect of a deconvolution filter is to compensate for the incident signal spectrum, which is probably severely band-limited and probably does not exhibit fine structure. If the filter is sufficiently long, however, compensation may be made for the fine structure produced by crustal effects.

For computational economy and real-time processing applications, it is desirable to design an "average" filter which will deconvolve an "average" teleseismic signal. The usefulness of such a filter depends upon the variability of signal spectra. All sources do not have the same characteristics, and transmission effects vary as functions of source-to-reciver travel path; unless the span of the deconvolution filter is more than a few seconds, however, it appears that differences in emergence angle will be unimportant. For example, Figure 2 shows the persistence of some fine structure (probably associated with Moho reflections) even when power spectra for 60 teleseisms of worldwide origin were averaged.

Figures 3 and 4 show the results of deconvolving five selected records. For each event, three deconvolution filters were designed from

- The autocorrelation function computed from a portion containing the P-phase of the record being filtered

- The average of autocorrelation functions for a subensemble of about 15 to 20 events (including the event to be filtered) having similar source-to-receiver distances
- The average of autocorrelation functions for all events in the appropriate ensemble

Table 3 lists source information for the five events. Impulse responses of the ensemble-average deconvolution filters are plotted in Figure 5.

Table 3

DESCRIPTIONS OF TELESEISMS DISPLAYED IN
DECONVOLUTION STUDY

Event No.	Source Region	Distance (°)	Depth (km)	Azimuth (°)	Magnitude (m _b)
I-4	Kurile Is.	85.99	50	324.0	4.9
II-39	Aleutian Is.	64.33	33	314.7	5.3
II-43	Chile	70.65	101	166.3	5.1
III-81	Chile	69.31	33	164.5	4.3
III-92	Greece	79.51	78	48.7	4.8

Although some crustal reverberation was probably achieved, deconvolution's most important effect was compensation for the incident signal spectrum. Since the signal-to-noise ratio was generally poor wherever signal power was low, this compensation generally tended to amplify noise more than signal. In order to maintain a good signal-to-noise ratio, the data shown in Figures 3 and 4 were high-cut-filtered at 1.5 cps in the playback operation. The playback filters possess smooth frequency response functions in their passbands. Therefore, it is reasonable to assume that any compensation by the deconvolution process for fine structure introduced by crustal reverberation should not be affected in the passband by the frequency filtering.

Deconvolution filter lengths were 5.4 sec, except for the 2.7 sec (individual deconvolution) and 1.95 sec (ensemble-average) of

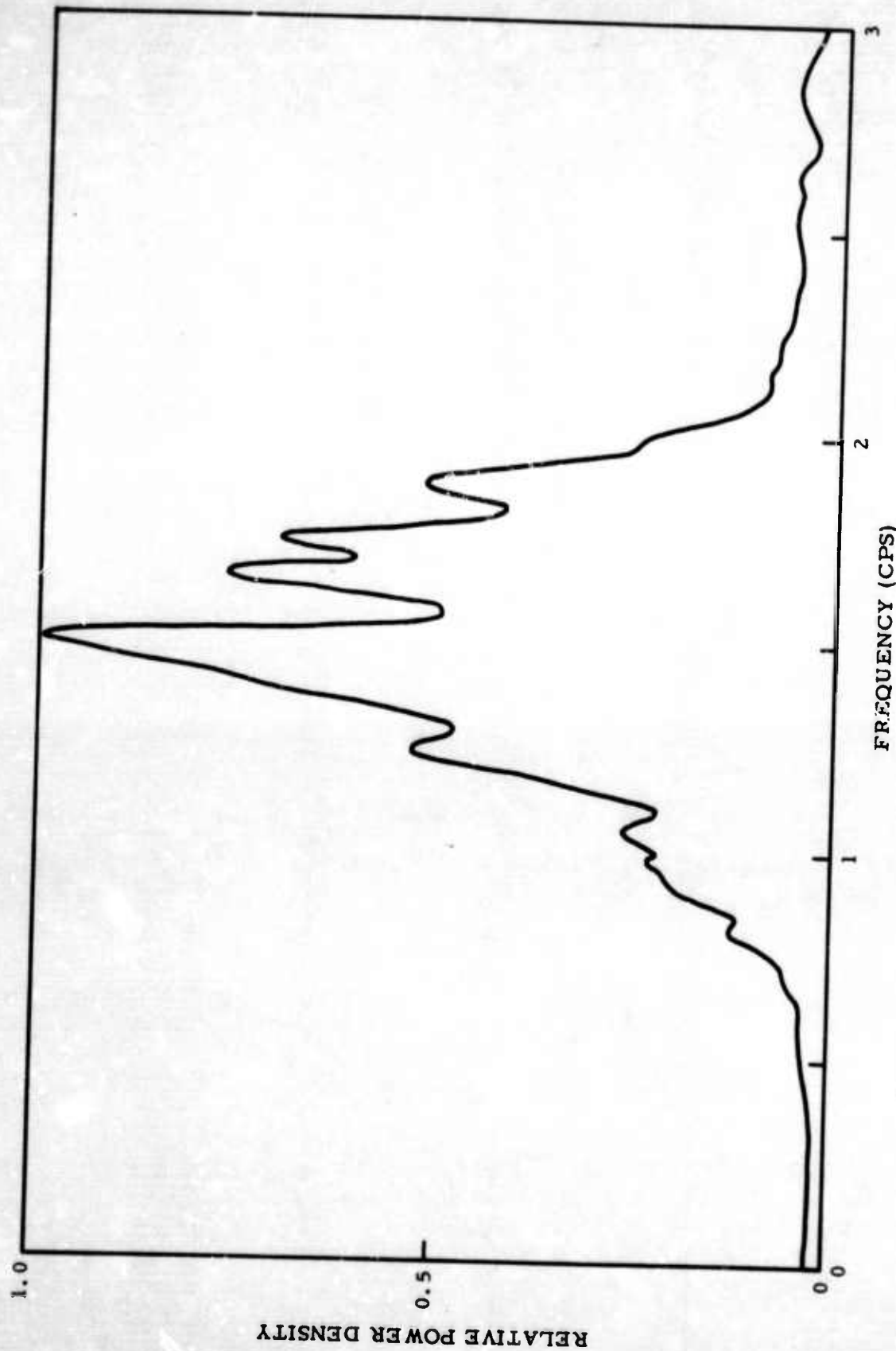


Figure 2. Average Power Spectrum of 60 Ensemble II Teleseisms

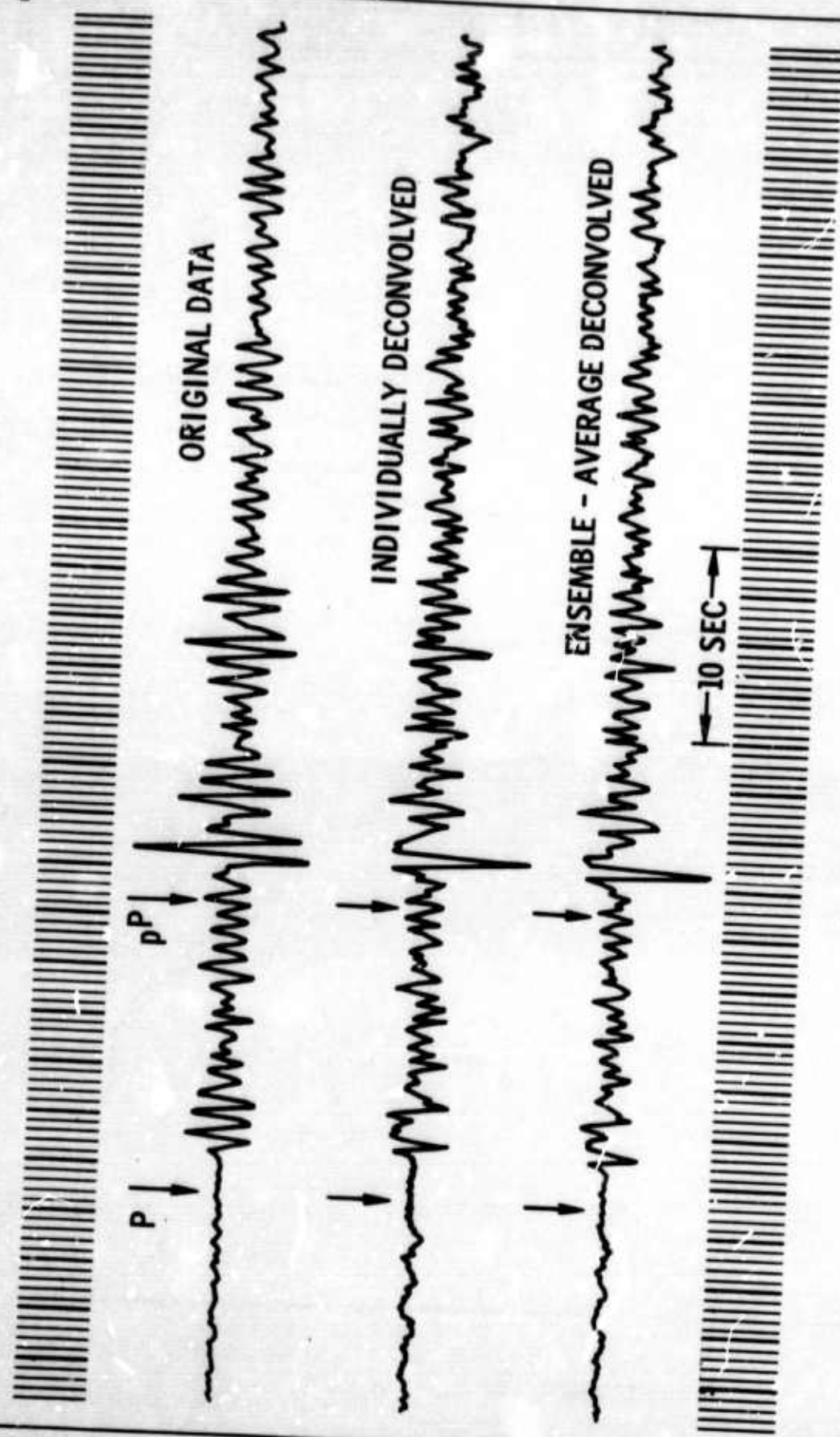


Figure 3. Original and Deconvolved Recordings of Event I-4 (1.5-cps High-Cut Playback Filter Applied)

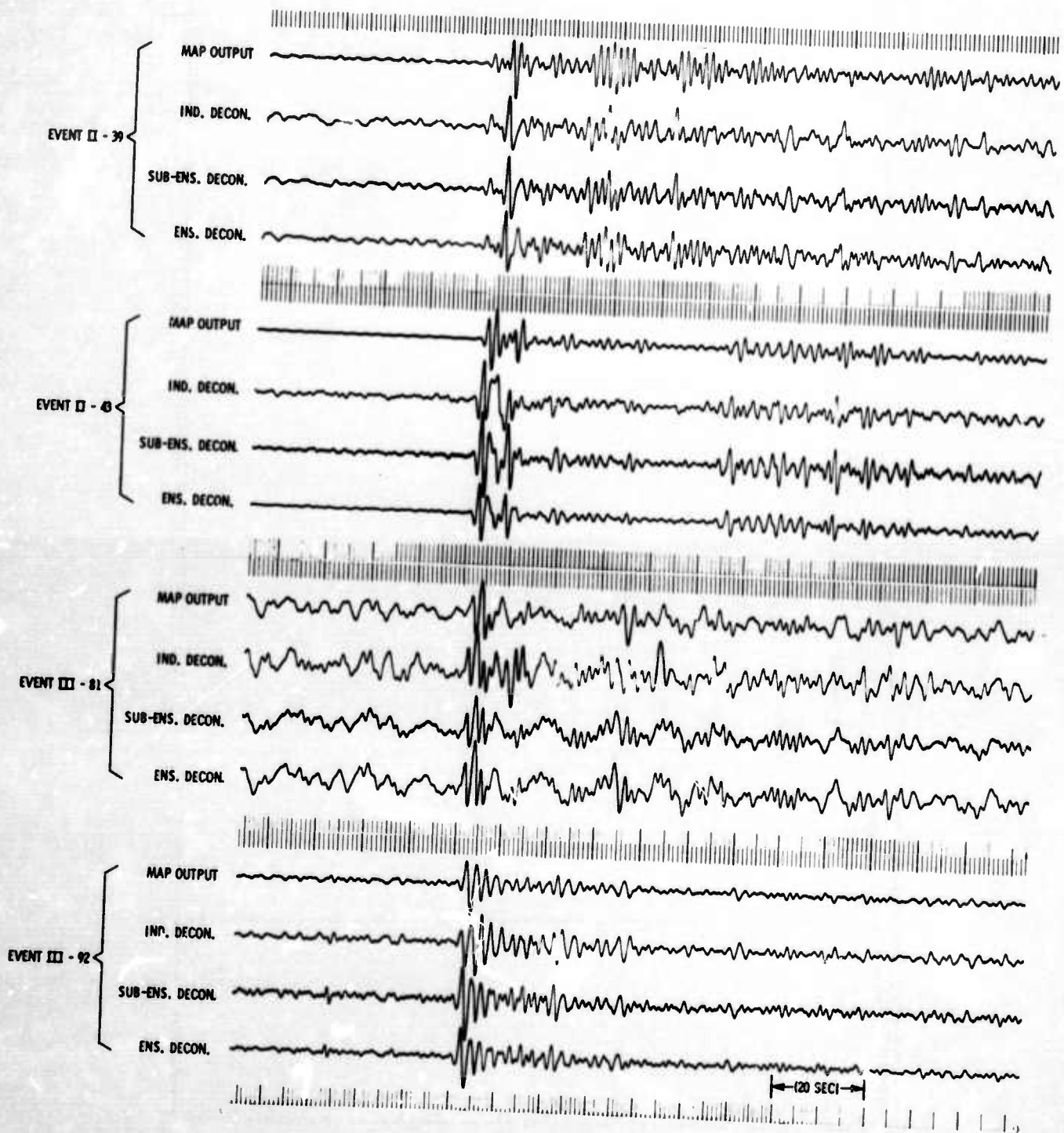


Figure 4. Original and Deconvolved Recordings of Four Events (1.5-cps High-Cut Playback Filter Applied)

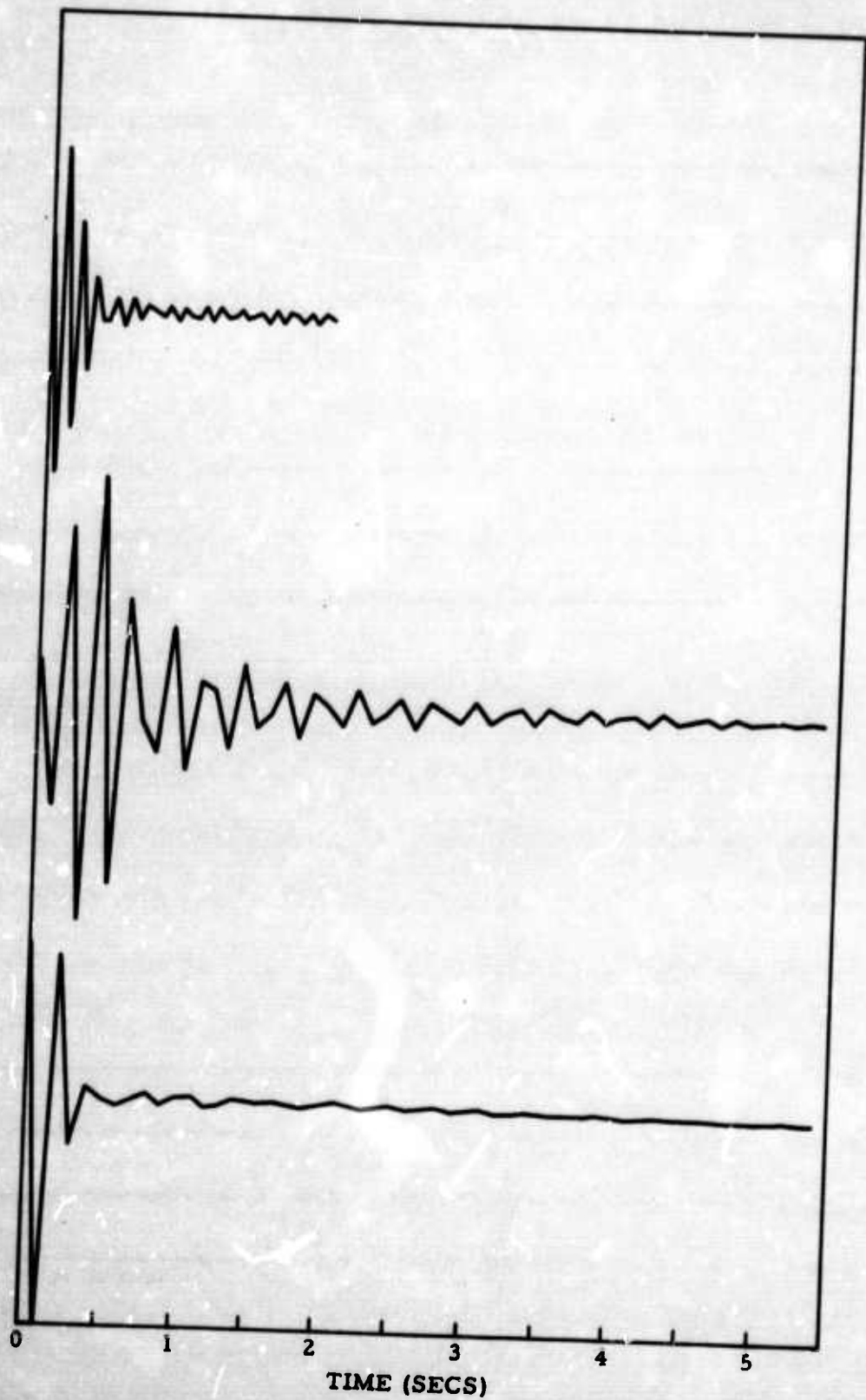


Figure 5. Impulse Responses of Ensemble-Average Deconvolution Operators



filters applied to event I-4. Thus, the filters were not sufficiently long to eliminate Conrad or Mohorovicic reflections, but times of reverberations in the sedimentary layers should be covered adequately.

The performance of the whitening filters is difficult to assess in any detail. It can be seen that P-waveforms are generally contracted somewhat, but it cannot be stated with certainty that this observation implies success in removal of crustal reverberation effects. Although the pP arrival is made sharper in some cases, no improvement in pP detectability as a result of deconvolution is observed. In general, little difference can be seen among the results of individual, subensemble-average and ensemble-average deconvolution of P-waveforms. This observation suggests that range-dependent effects are not very important and that a single "average" deconvolution operator should be adequate for real-time online processing at an array site. *

* Note, however, that results given in Section VI imply that a separate deconvolution operator for core phases would be desirable. The ensemble-average filters described above were designed mainly from P-phase statistics and were applied only to direct P-events.



SECTION IV

DEPTH-OF-FOCUS DETERMINATION

An accurate estimate of focal depth can be of value for discrimination between earthquakes and nuclear explosions, since it may be assumed that man-made events must be confined to shallow depths.

Focal depths of earthquakes are determined most often by least-mean-square fits to observed arrival times of P. An alternate method depends upon the difference in observed arrival times of P and pP. The (pP - P) method probably is more accurate, but it requires that pP be observed and identified with certainty. The value of multi-channel velocity filtering of seismometer array outputs has been demonstrated in that it has sometimes been possible to identify pP in the output trace of the CPO processor when it was not observable in single-seismometer records. In other cases, however, pP could not be seen even when its predicted arrival time was favorable for observation (i.e., when USC&GS-estimated focal depth indicated that pP should arrive after P had died out, but before the end of the record).

It has been suggested that it might be possible to improve pP detectability by deconvolving the processor output record or by computing autocorrelations for either the raw trace or the deconvolved trace. It can be seen from Figures 3 and 4 that deconvolution does not always sharpen the pP waveform; in some rare cases, in fact, pP is more difficult to find in the deconvolved record than in the original record.

If the waveform of pP were similar to that of P, the autocorrelation of a teleseism would be expected to display a marked peak at the time lag corresponding to the difference in arrival times of the phases. It was therefore suggested that autocorrelation functions might provide a method of detecting the pP phase of weak events for which reliable identifications could not be made from the seismograms. In most cases, however, it was not possible to determine the (P - pP) delay from the autocorrelations of either raw or deconvolved records (Figure 6), even when pP could be definitely identified in the corresponding seismogram. (The autocorrelations were filtered by a 5-point moving average in order to facilitate interpretation by removing high-frequency noise.)

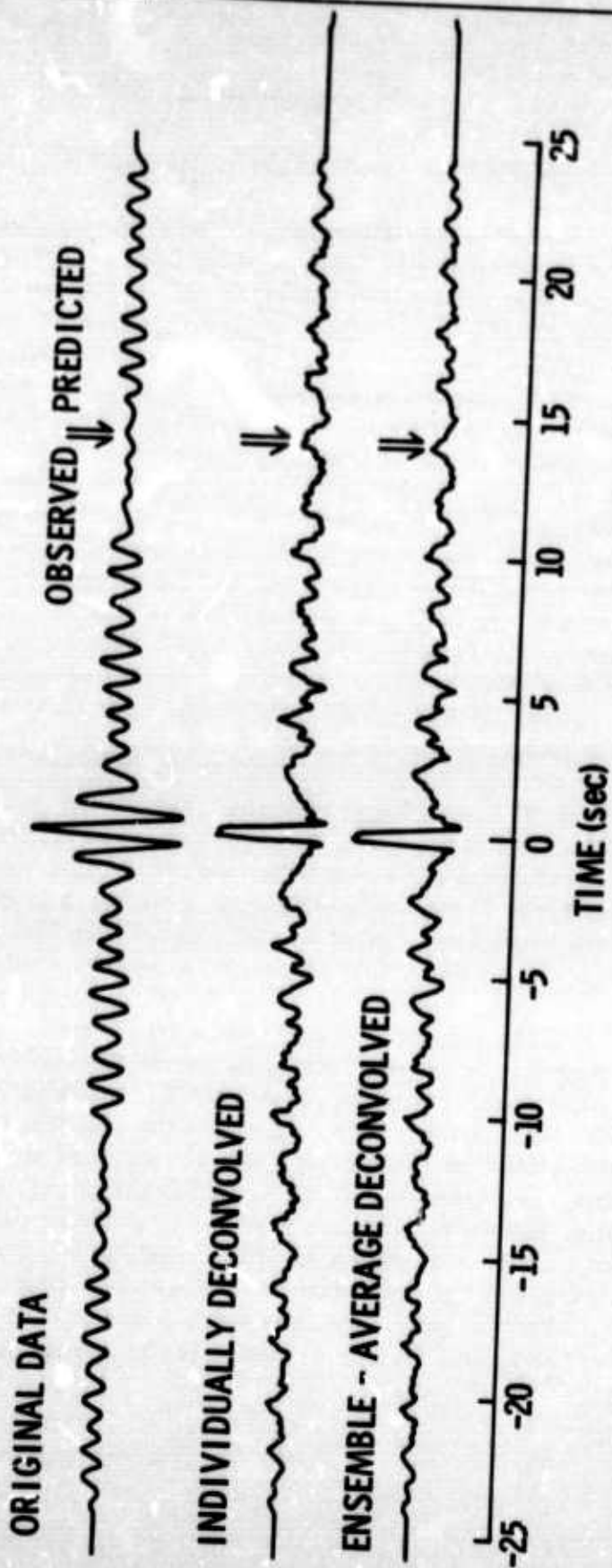


Figure 6. High-Cut-Filtered Autocorrelations of Original and Deconvolved Records of Event I-4, with Observed and USC&GS-Predicted P-pP Intervals Indicated



The failure of deconvolution and autocorrelation methods to improve the detectability of pP is attributed to differences between the waveforms of P and pP from the same events. Some shaping of pP is to be expected during its passage through the crust above the source, but it is felt that this effect is of minor importance; otherwise, the travel paths of P and pP are essentially the same. A more reasonable explanation is asymmetry of the radiation pattern of the source so that the original waveform of the signal traversing the P travel path is substantially different from that following the pP path.

It must be concluded that (pP - P) analysis is of limited value in focal depth estimation for earthquake/explosion discrimination. A well-documented pP phase offers excellent proof that focal depth was greater than a few kilometers; however, several deep-focus events (USC&GS-estimated depth > 100 km) did not produce observable pP arrivals. A possible explanation has been suggested above. Regardless of the reasons, it must be concluded that pP absence cannot now be accepted as evidence of near-surface origin.



SECTION V

STUDY OF CPO CRUSTAL STRUCTURE

Two important effects must be considered when trying to deduce the crustal structure beneath CPO from the analysis of teleseismic records.

First, since crustal response depends on signal angle of emergence, a single average response function estimate for the complete set of teleseisms has no meaning. In the case of Ensemble I, 73 events from a small range of distances and azimuths are available. By forming seven different subgroups and computing average autocorrelations (Figure 7), it is possible to find "events" in the autocorrelation functions which are interpreted as evidence of major reflecting horizons below CPO. Such "events" no longer appeared when ensembles of worldwide origin were averaged.

Second, observed spectra can be interpreted as crustal response functions only after they have been corrected for spectral content of the original signal incident at the base of the crust. For this reason, interpreting the responses of deconvolution filters (Section III) as the inverse of the crustal response is not meaningful. No significant "events" could be observed in average autocorrelations of subensembles of Ensembles II and III, even when the subgroups covered distance ranges as small as 10° . Evidence of reflections was cancelled beyond recognition, probably because of differences in signal spectra. Figure 8 illustrates the great diversity observed in teleseisms from a small range of distances. Power spectra have been computed for 18 Ensemble II events between 20° and 30° . It can easily be demonstrated that these differences are associated with the signals, since noise power spectra (Figure 9) computed for intervals just preceding each event show excellent time-stationarity. It is believed that the observed differences in signals at nearly the same distance away may be explained by near-source effects. It should be possible to average out these effects to some extent by the use of large numbers of teleseisms.

In Ensembles II and III, it is not possible to obtain such a concentration of foci. It appears that the most effective method of eliminating source effects might be to discard all shallow-focus events. As an example, power spectra for seven deep-focus events (II-21 and III-25 through III-30) are shown in Figure 10; it has not been possible to find such striking resemblances in similar groups of shallow-focus events. In Figure 11, autocorrelations of four teleseisms (III-27 through -30) show

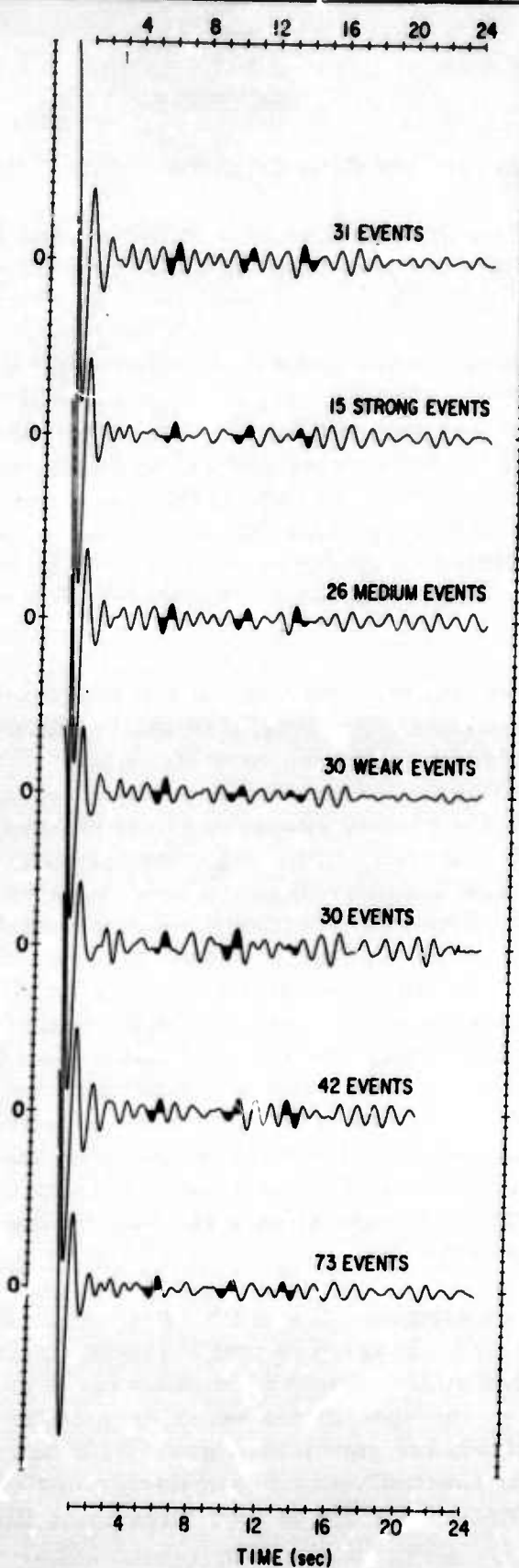


Figure 7. Average Autocorrelations of Subgroups of Ensemble I Events

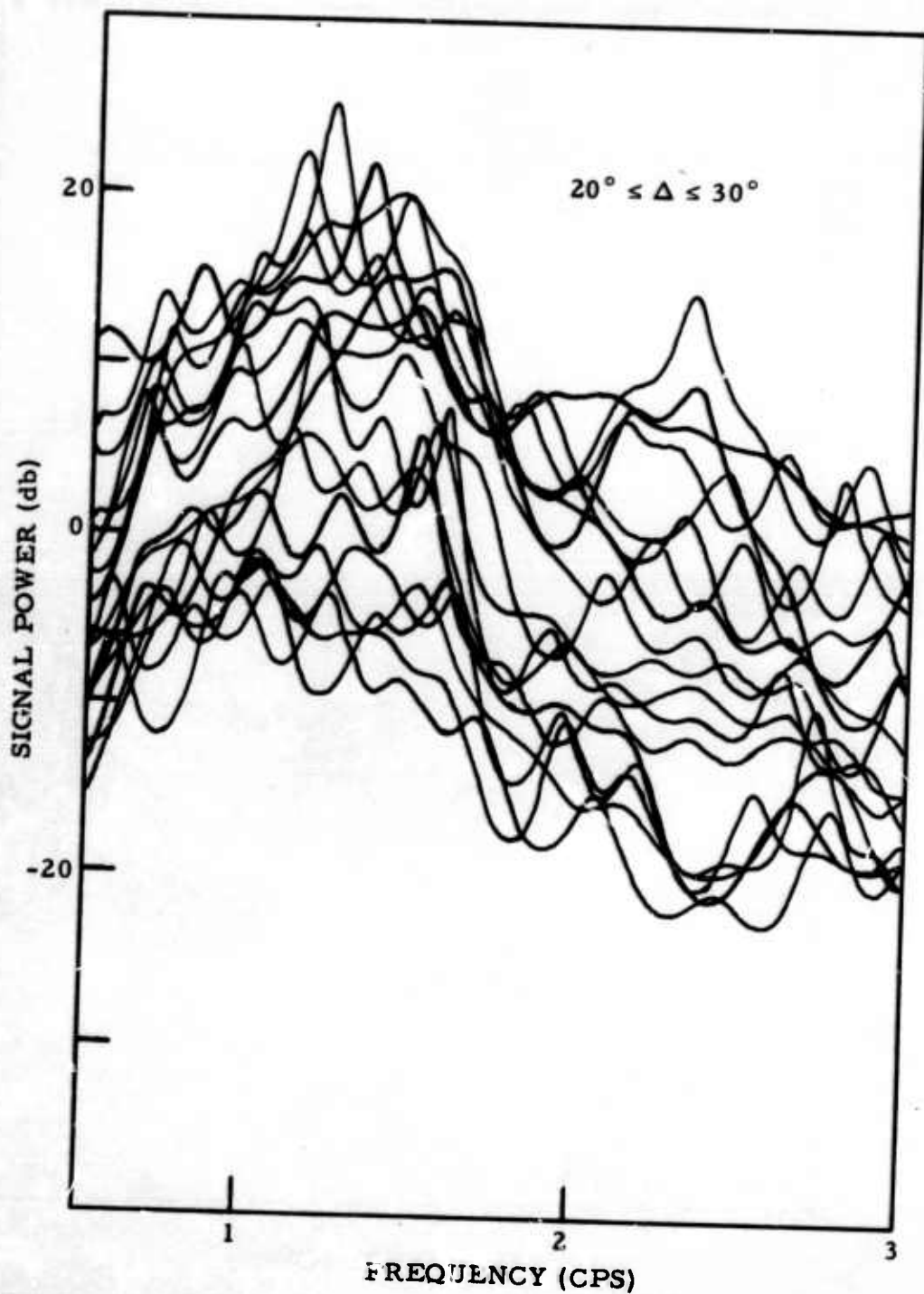


Figure 8. Signal Power Spectra of 16 Ensemble II Events Between 20° and 30°

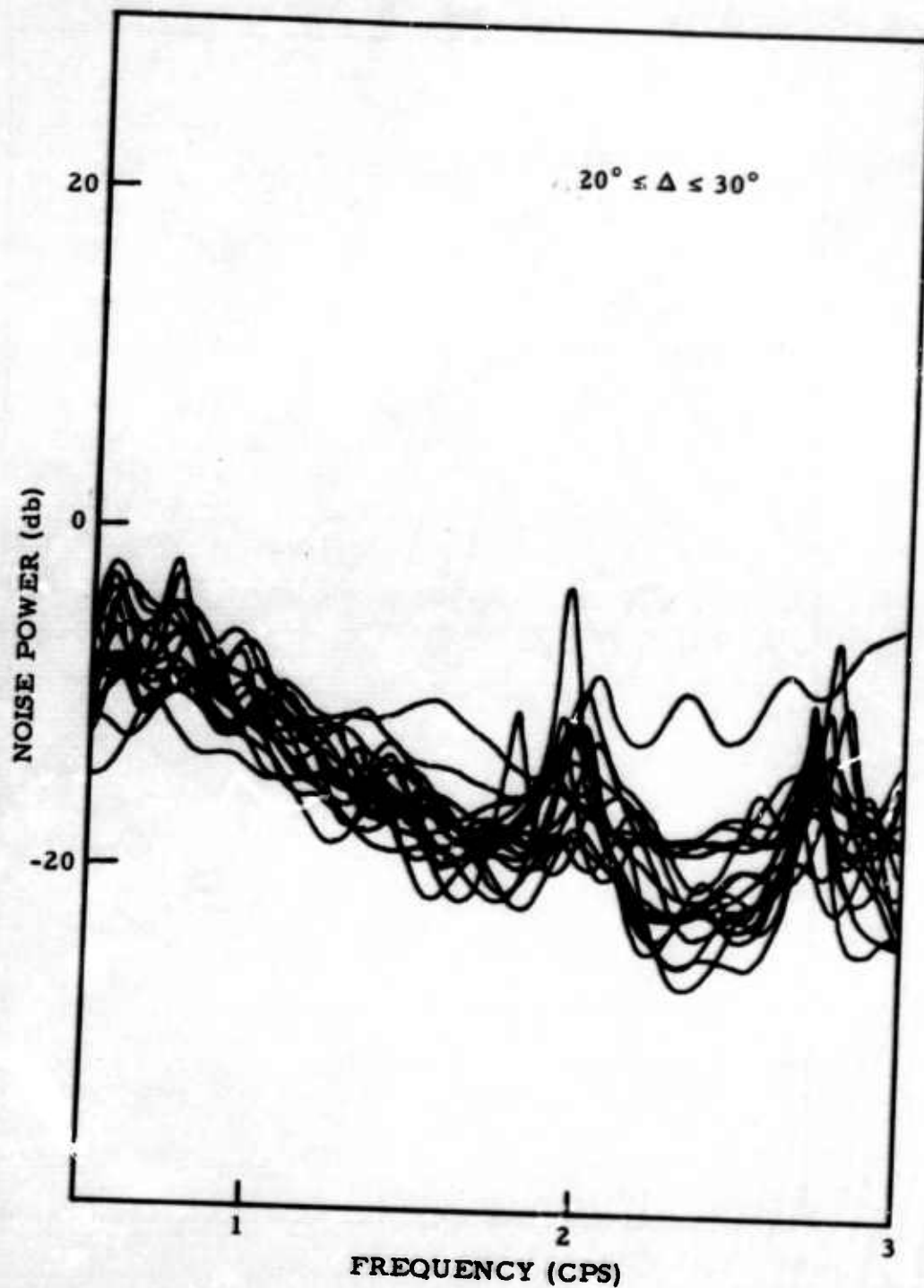


Figure 9. Noise Power Spectra Associated with 18 Ensemble II Events
Between 20° and 30°

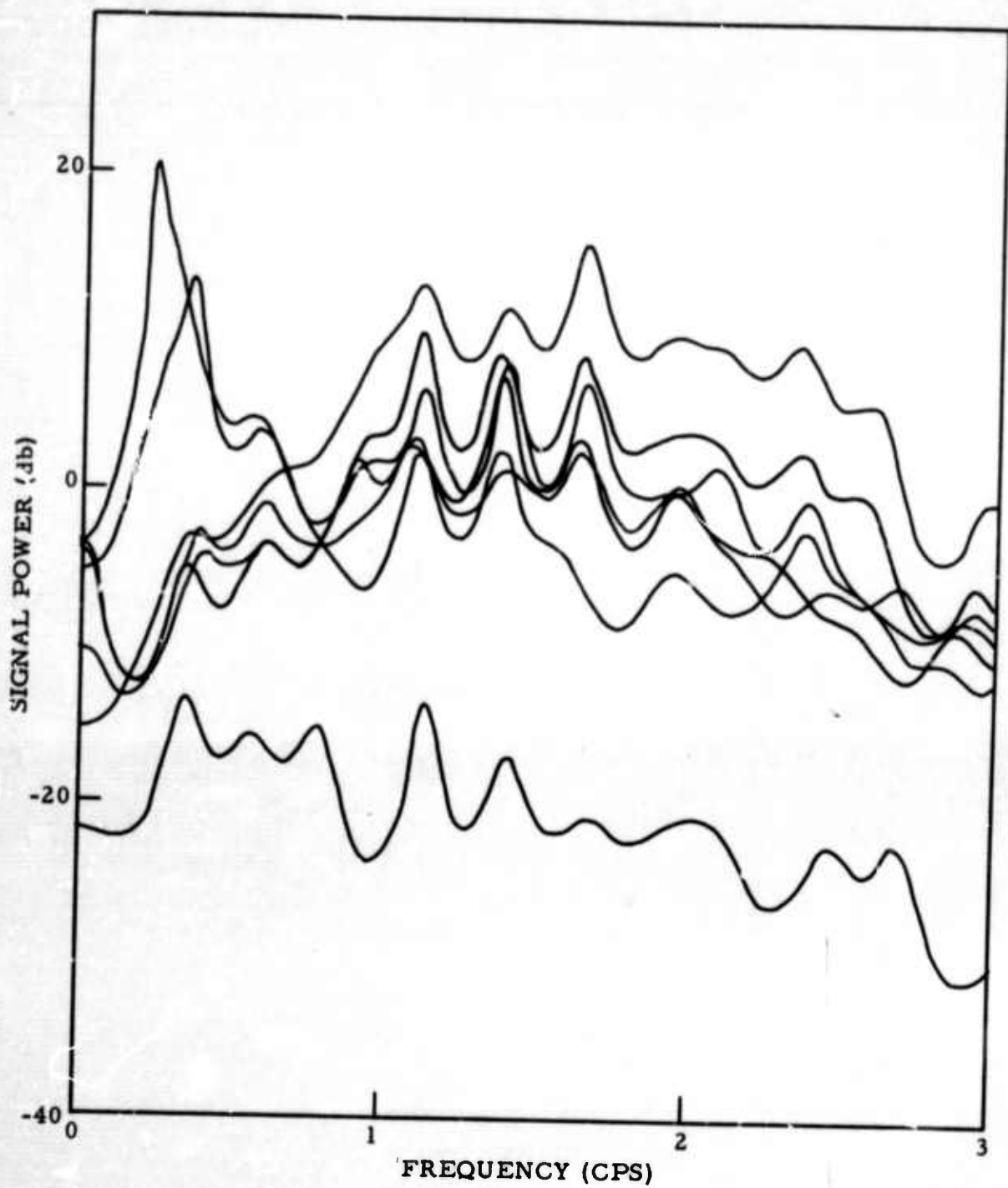


Figure 10. Signal Power Spectra of Seven Deep-Focus Events Between 30° and 31.3°

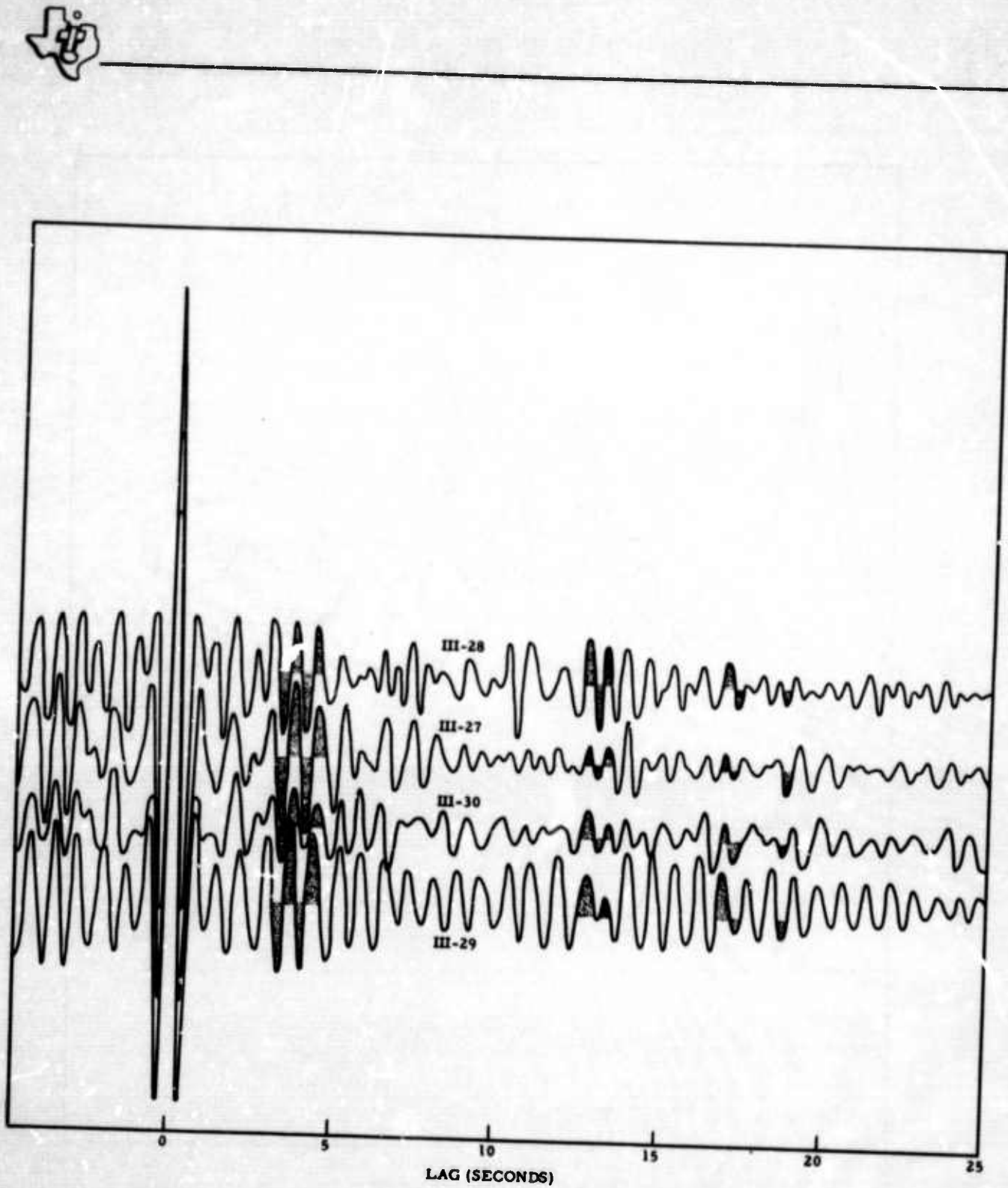


Figure 11. Autocorrelations of Four Teleseismic Signals from Earthquakes Near the Colombia-Venezuela Border



four "events" which are reproducible throughout the set. A thorough study of the available data unfortunately has failed to turn up any other sets which display such similarities. The four earthquakes which contributed to Figure 11 occurred at distances of 30.9° , 30.73° , 31.33° , and 31.01° , with azimuths between 155.1° and 155.6° and focal depths between 140 and 176 km. This was the only available set of deep-focus earthquakes from such a small area.

A major difficulty in interpreting the autocorrelations and power spectra in terms of crustal structure arises from the limited bandwidth of the signals being studied. Since most signals have useful bandwidths of about 1 cps, the finest resolution obtainable is about 1 sec of time or a few kilometers of depth. A suggested model for the structure under CPO is reproduced in Figure 12.⁹ Since the 2-way travel time through the entire sedimentary section is only 1.05 sec for this model, it is impossible to learn anything about detailed structure in the sediments and very difficult to determine even their total thickness. Ideally, autocorrelation functions should exhibit peaks at time lags corresponding to the differences in arrival times of direct and reflected signals. The correlations in Figures 7 and 11 are computed from signals with phase velocities of 22.5 km/sec (Kurile Islands, 85° ; and 12.6 km/sec (Colombia-Venezuela, 31°). The difference in phase velocities should produce shifts of the peaks in the autocorrelations.

Some events that are multiply-reflected and are most likely to contain significant energy are illustrated in Figure 13. The time lags of these events, relative to the direct P-wave, are given in Table 4 for the crustal model of Figure 12. Some features in the autocorrelations have been selected as evidence of reflected arrivals, but it is difficult to decide upon the proper lag times which should be assigned to such features. Ideally, a reflected arrival should give rise to a reproduction of the center part of the autocorrelation; the reproduction should be symmetrical and centered at the lag time of the arrival. Therefore, it is preferable to seek center times rather than onset times of the "events." Since most of the "events" selected are asymmetrical, center times are difficult to estimate. The added complication of limited signal bandwidth implies that optimum resolution is between 1 and 2 sec.

Estimated times for the first two "events" in Figure 7 are 6.0 sec and 10.5 sec. These probably represent events B and A with 22.5-km/sec phase velocity. If this identification is correct and the lag times have been estimated accurately, then the depths of the Conrad and Mohorovicic discontinuities as given in Figure 12 are too large by about 2 km.

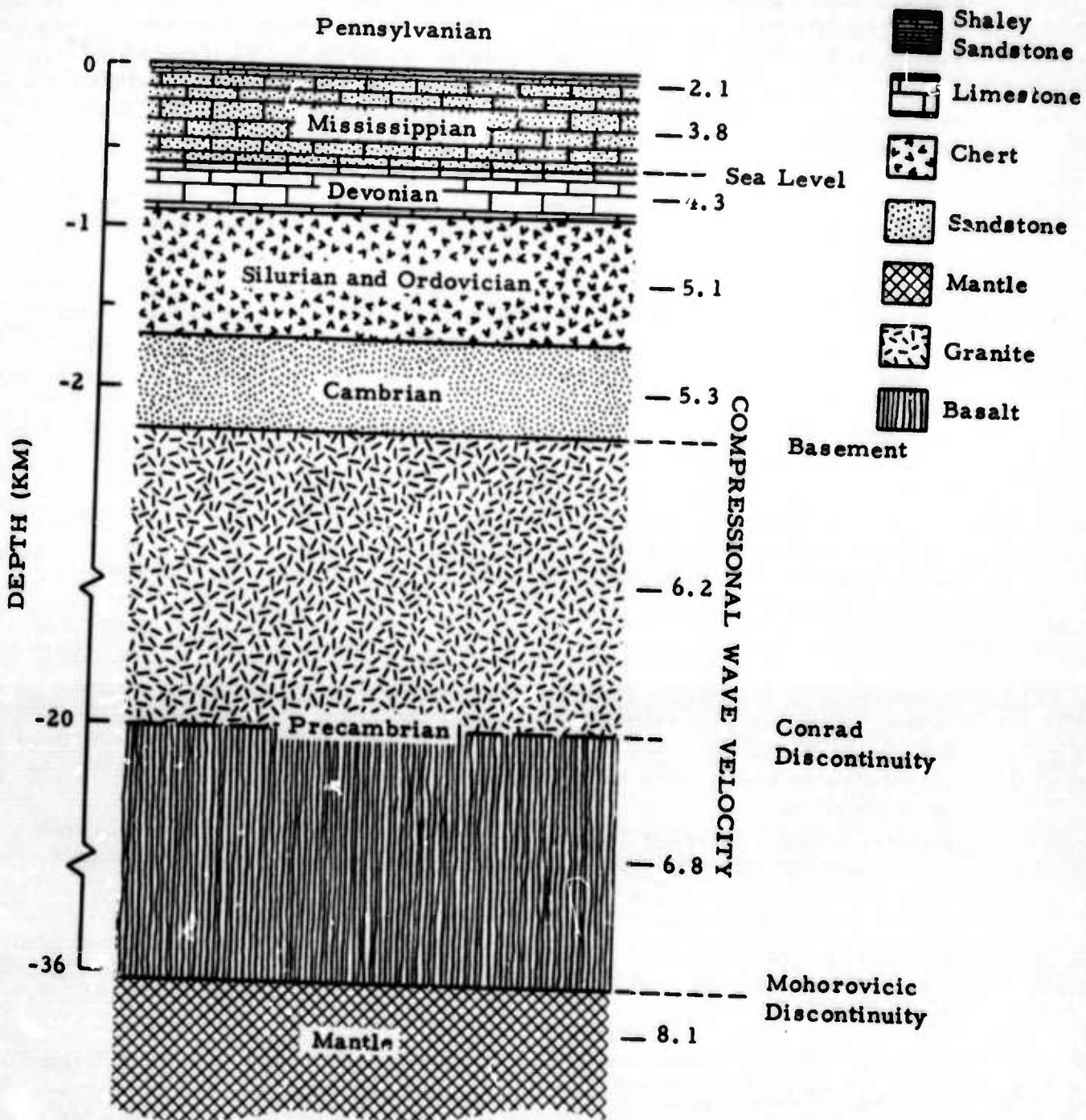


Figure 12. Model of Crustal Structure Near McMinnville, Tennessee

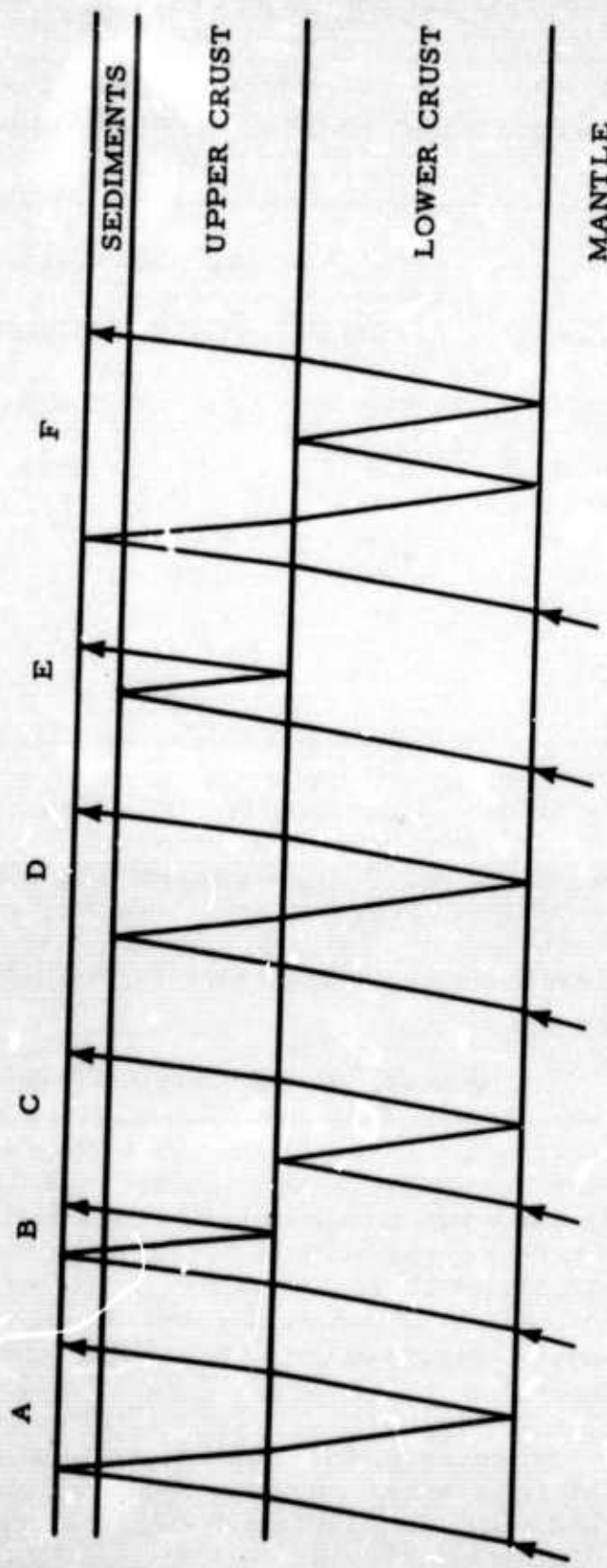


Figure 13. Travel Paths of Reflected Arrivals



Table 4
COMPUTED LAG TIMES OF REFLECTED ARRIVALS

Signal Phase Velocity (km/sec)	Lag Time (sec)					
	Arrival A	Arrival B	Arrival C	Arrival D	Arrival E	Arrival F
12.6	10.0	6.0	4.0	9.0	5.0	14.0
22.5	11.0	6.5	4.5	10.9	5.5	15.5
∞	11.5	6.8	4.7	10.4	5.7	16.2

However, the dominant near-surface reflector could be an interface within the sedimentary section or even the base of the sediments, in which case the predicted Conrad and Mohorovicic depths would be too small by about 2 km. The "event" found near 15 sec could be any one of a large set of multiply-reflected arrivals; but event F seems to be the most likely arrival. The ambiguity in interpretation remains, since the apparent error in lag time can be removed either by decreasing the Conrad and Mohorovicic depths or by assuming the dominant near-surface reflector to be the base of the Devonian.

In Figure 11, "events" have been found at 4.2 and 12.9 sec for a phase velocity of 12.6 km/sec. The major peaks in Figure 10 occur at intervals of 0.28 cps, implying a reflecting system with a lag time of 3.6 sec. The differences in the lag times found for 22.5 and 12.6 km/sec are much greater than would be expected unless different reflecting interfaces predominate in the two cases. It is difficult to conceive how a model consistent with Figure 12 could give rise to only the "events" seen in Figure 11. Since the four earthquakes contributing to Figure 11 were so similar, it may be that the observed coincidences can be attributed to source effects.

In summary, the results suggest that the assumed crustal model for CPO is not in error by more than 1 or 2 km, but the results are not of sufficient quality to permit more definite conclusions at this time.



SECTION VI

INVESTIGATION OF PROPAGATION MECHANISMS

An attempt was made to use the high-quality teleseism records from the CPO processor to examine such subjects as anelastic absorption in the earth's interior and the dependence of crustal response on source range and azimuth. More than 100 different groups of events were chosen from Ensembles II and III on the basis of range, azimuth, focal depth, magnitude, and observed signal-to-noise ratio. Autocorrelation functions and power spectra were computed for each subensemble.

A striking range dependence has been observed, but examination of the data has failed to turn up evidence of characteristics which can be shown to vary systematically with any other of the parameters listed above. It is suggested that, because of the large number of variables involved (e.g., focal depth, geographical location of source, source-to-receiver distance and azimuth, geological source environment, source spectrum, magnitude, continental or oceanic nature of early part of travel path, source radiation pattern, etc.), the number of available recordings is too small to provide useful statistical significance. The chief difficulty seems to be that, with only a single receiver array, it is impossible to separate source effects from transmission effects. Whereas seismic sources may be highly variable, differences in transmission effects from event to event are relatively subtle. It is believed that, with a sufficiently large collection of recordings, it should be possible to estimate the characteristics of an "average" source for each combination of values of range, azimuth, etc. However, it is felt that a more satisfactory method of eliminating source effects would be the use of a group of arrays, each array recording signals associated with the same events.

Figure 14 shows average smoothed power spectra computed for subgroups of Ensemble III; each subgroup is comprised of a particular range of source-to-receiver distance (distances in degrees of arc along a great circle). For distances less than 110° , the behaviour of the observed spectrum is characterized by a gradual shift of the peak frequency from high to low frequencies with increasing distance. Between 110° and 120° , a change of character is observed. Instead of continuing to increase in importance, the low-frequency part of the signal is seen to wane to the extent that energy density measured at 0.25 cps is only about 14 percent (-8.5 db) of that measured in the neighborhood of 1.25 cps. Also, the spectral peaks are observed to be much broader beyond 120° than at shorter distances.

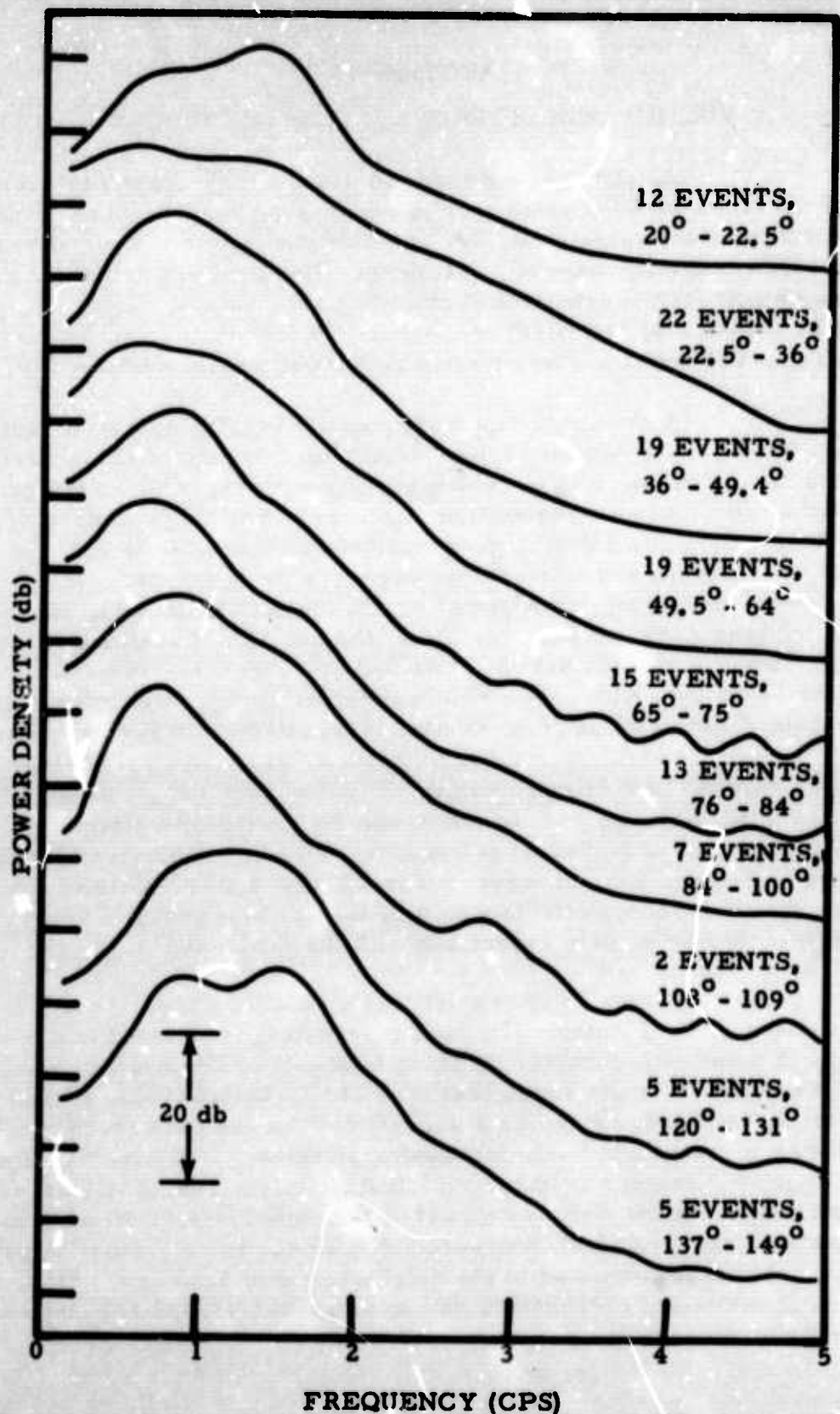


Figure 14. Smoothed Average Power Spectra of Ensemble III Events
Grouped According to Distance



The subgroups of Figure 14 were chosen so that the first seven subensembles contain direct P-phases, subensemble 8 contains one diffracted P and one PP, subensemble 9 contains PKIKP arrivals, and subensemble 10 contains a mixture of PKIKP and PKP events. (See Figure 15 for a definition of these phases in terms of ray paths.) The observed lack of low-frequency energy appears to be, at least for the ensemble being studied, a unique quality of core phases, since it is not observed in P, diffracted P, or PP events.

It is possible that the observed effect may be a characteristic of the source region or of the azimuth of arrival at CPO. The portion of the circum-Pacific seismic zone between Alaska and Indonesia does not deviate very much from a great circle passing through CPO. Of the PKP and PKIKP events observed, 80 percent originated in the circum-Pacific belt and had azimuths between 295° and 340° , whereas only 26 percent of the P arrivals are associated with azimuths between 295° and 340° .

Figure 16 shows average power spectra for subgroups of events, each subgroup corresponding to a small range of source locations. All events with azimuths outside the range 305° to 356° have been eliminated (Table 5). The characteristics seen in Figure 14 persist when only circum-Pacific earthquakes are considered, although they are somewhat less obvious because of poorer statistics. It would be desirable to prepare similar displays for other azimuths, but sufficient data were not available. Therefore, it is not possible to determine whether the observed effect is a general one or simply a quality of circum-Pacific earthquakes as seen at the CPO station.

No previous observation of this phenomenon has been found in the published literature. In their classic paper, Gutenberg and Richter⁴ stated that frequencies greater than 0.5 cps are generally observed only in the purely compressional phases P, PP, and P'. (The symbol P' was used to designate both PKP and diffracted P.) In particular, it was indicated that the "diffracted P' ($\Delta < 142^{\circ}$)" is distinguished by a marked prevalence of high frequencies; whereas, the "true P' ($\Delta > 142^{\circ}$)" seldom contains much high-frequency energy, the most common observed peaks being about 0.1 cps, with a number at 0.2 cps and only a few observed at 0.5 cps. On the contrary, the CPO events display higher peak frequencies for PKIKP and PKP phases than distant P phases.*

* Before the recognition of the effect of the inner core, it was believed that diffracted P was the only simple phase which could be observed in the "shadow zone" between 103° and 142° . Although diffracted P is the first arrival at distances out to 142° , the energy of this phase decays rapidly with increasing distance, and PKIKP was always the first observable phase of Ensemble III events from distances between 110° and 142° .

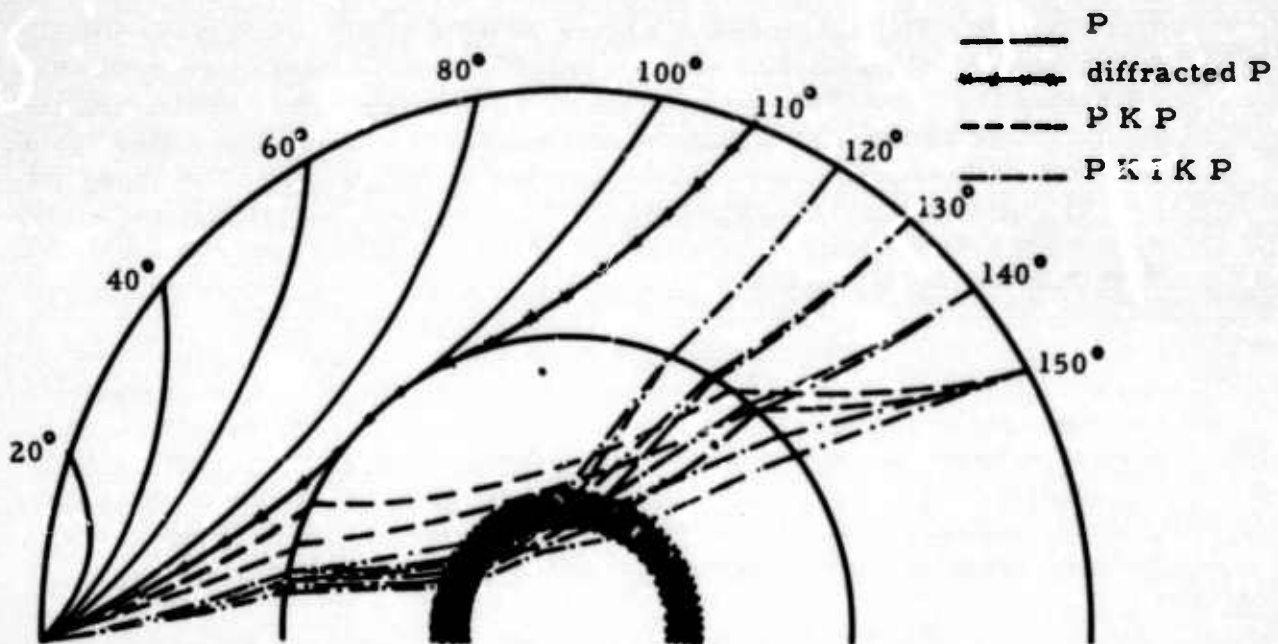


Figure 15. Ray Paths of Compressional Waves in the Earth's Core and Mantle

Gutenberg (1959, p. 111)³ states that, at epicentral distances between about 125° and 140°, waves with frequencies of 1 to 2 cps arrive about 10 to 20 sec earlier than the definite PKIKP impulse with frequencies of about 0.5 cps or less. This dispersion effect cannot be used to explain the observed lack of low-frequency energy since the power spectra were computed from data samples sufficiently long (3 min) to include late-arriving energy and since Gutenberg states that the high-frequency part of the PKIKP is generally very weak compared to the low-frequency part.

At this time, no explanation can be suggested for the lack of low-frequency energy in the core phases. Because the difference between P-phase spectra and core-phase spectra is so striking, it should follow that a single deconvolution filter cannot be appropriate for both direct P events and events transmitted through the core.

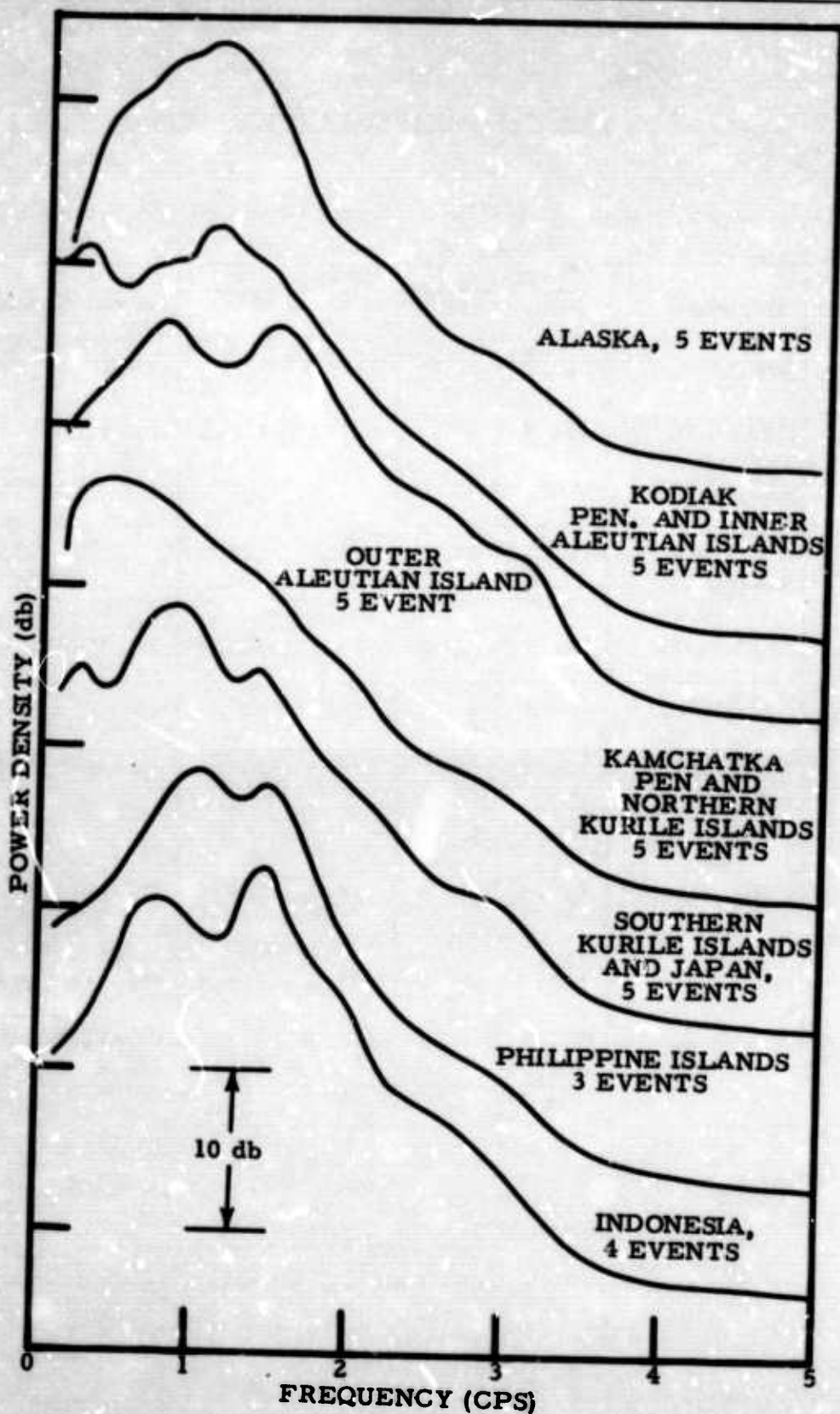


Figure 16. Smoothed Average Power Spectra of Circum-Pacific Events Grouped According to Source Region

Table 5
CIRCUM-PACIFIC EARTHQUAKES

Subgroup No.	Location	Range of Distances (°)		Range of Azimuths (°)		Event Numbers
		Min.	Max.	Min.	Max.	
1	Alaska	46.1	49.5	316.9	326.5	45, 46, 48, 49, 54
2	Kodiak Pen. and Inner Aleutian Is.	54.1	59.2	314.5	316.4	60, 61, 62, 63, 66
3	Outer Aleutian Is.	62.7	66.7	315.4	316.9	71, 72, 73, 75, 76
4	Kamchatka and Northern Kurile Is.	71.8	83.0	322.7	326.8	83, 85, 86, 96, 97
5	Southern Kurile Is. and Japan	86.5	99.1	325.4	329.6	102, 103, 104, 105, 107
6	Philippine Is.	120.4	126.9	319.0	331.2	110, 111, 112
7	Indonesia	141.7	148.7	305.8	356.4	116, 117, 118, 119



SECTION VII

COMPARISON OF PROCESSORS AT CPO

In Figures 3 and 4, samples of seismic noise occurring just before the F onset have been preserved. Visual examination of these recordings and of other events not displayed in this report permits a qualitative evaluation of the performances of processors IP-1 and IP-8.

As seen in the recordings of Ensemble III events, the processor IP-1 permitted a large fraction of the surface-wave noise to pass into the output. The level of the noise is found to vary over a range of more than 10 db from trace to trace. The high noise power observed on some records, e.g., event III-18, suggests intermittent microseismic storms.

By contrast, the noise observed on the Ensemble II records is remarkably time-stationary, as is shown by the noise power spectra in Figure 9. It is hypothesized that, because IP-8 and the low-cut filters were so much more efficient at rejecting surface-wave noise, the noise which was passed was composed mainly of P-waves and the intensity of this background of P-wave noise did not fluctuate much. These results imply that a detector employing decision-making equipment should be able to operate effectively on the output of an array processor such as IP-8 which is capable of rejecting surface-wave noise efficiently.



SECTION VIII CONCLUSIONS

Through the analysis of recordings put out by MAP systems at CPO, it has been possible to undertake studies which are uniquely dependent upon having cleaned-up signatures of teleseisms.

Deconvolution filters designed from experimental signal statistics have been used to sharpen the waveforms of some events. It was found that filters designed from average correlation properties of groups of signals were virtually as effective in sharpening most signals as filters designed from the individual signals (except that core phases were found to be significantly different from direct P-phases). It is believed that the primary effect of the filters studied was to compensate for nonwhiteness of the source spectrum and that the removal of crustal reverberation effects was of minor importance.

Detectability of later phases such as pP generally was not improved by deconvolution filtering, and it was not possible to find evidence of pP in autocorrelation functions computed either before or after deconvolution. The failure of these analytical techniques for pP identification (and hence depth-of-focus estimation) is attributed to differences between the P and pP waveforms caused by asymmetric source radiation patterns. Therefore, it is impossible at this time to designate events as of definite near-surface origin on the basis of absence of an observable pP phase.

Autocorrelation functions and power spectra computed from recorded signals were studied in order to investigate the crustal structure below CPO. The limited signal bandwidth limits resolution to a few kilometers. The only sound conclusion which can be drawn is that a previously proposed model of the crust is probably not in error by more than 2 km.

Attempts to investigate mantle transmission mechanisms through observed signal autocorrelations and power spectra were unsuccessful.

A deficiency of low-frequency energy was observed in signals which had traveled through the earth's core, but a propagation mechanism accounting for this effect has not been found. It was concluded that subtle variations in transmission effects were masked by large variations in source characteristics. Source effects could best be overcome by the use of several receiver arrays, each recording signals produced by the same events.

SECTION IX

REFERENCES AND BIBLIOGRAPHY

1. Cleary, J. R. and A. L. Hales, 1966, Azimuthal variations of U.S. station residuals: *Nature*, v. 210, p. 619-620.
2. Gutenberg, B., 1945: Magnitude Determination for Deep-Focus Earthquakes, *Bull. Seism. Soc. Am.*, v. 35, p. 117-130.
3. Gutenberg, B., 1959: *Physics of the Earth's Interior*, Academic Press, New York.
4. Gutenberg, B. and C. F. Richter, 1935, On seismic waves, 11: *Gerlands Beitr. Geophys.*, v. 45, p. 280-360.
5. Jeffreys, H. and K. E. Bullen, 1958: *Seismological Tables*, Pub. of British Assn., London.
6. Texas Instruments Incorporated, 1963a: Synthesis and Off-Line Evaluation of a Multichannel Filter System Designed from a Theoretical Model of Signal and Noise for the Enhancement of Mantle P-Waves, AFTAC Contract AF 33 (657)-12331, 15 Sept.
7. Texas Instruments Incorporated, 1963b: Synthesis and Evaluation of Six Multichannel Filter Systems Based on Measured Correlation Statistics of Ambient Noise at Cumberland Plateau Observatory Designed to Operate on Rings of Seismometers, AFTAC Contract AF 33 (657)-12331, 31 Dec.
8. Texas Instruments Incorporated, 1964a: Synthesis and Evaluation of a Nineteen-Channel Filter System for the Extraction of Teleseismic P-Waves from Ambient Seismic Noise at Cumberland Plateau Seismological Observatory, AFTAC Contract AF 33 (657)-12331, 20 Jan.
9. Texas Instruments Incorporated, 1964b: Some Theoretical Calculations on a Model of the Crust under the Cumberland Plateau Observatory, Unpub. by J. Foreman.
10. Texas Instruments Incorporated, 1964-1966: Semiannual Technical Reports No. 1, 15 May 1964; No. 2, 15 Nov 1964; No. 3, 3 Jun 1965; No. 4, 15 Dec 1965; No. 5, 1 Jul 1966, AFTAC Contract AF 33(657)-12747.